switching device capabilities, e.g. due to switching losses and dead time distorting the output voltage.

2. Analysis of SPWM Control for UPS Inverter

Sinusoidal PWM, also known as sub harmonic or sub oscillation modulation is a carrier-based voltage control method. Its purpose is to synthesize the switch gating signals in such a way that the output voltage or current waveform is as close to a sinusoid as economically possible. Naturally sampled SPWM with triangular carrier is considered in this paper.

Basically, a sine reference wave, serving as modulating signal, is compared with a triangular carrier wave, and the intersection points determine the switching angles and pulse widths as in Figure 2. The generated switch gating pulses vary proportionally with the modulating (control) signal; in other words, the pulse width is maximum in the middle of each half period and decreases as cosine function towards either side. The frequency of modulating signal f_o determines the inverter's output and its peak amplitude A_m controls the modulation index

$$M = \frac{A_m}{A_c} \tag{1}$$

where A_c is the amplitude of carrier signal.

The frequency modulation index is:

$$M_f = \frac{f_c}{f_o} \tag{2}$$

where fc is the carrier frequency

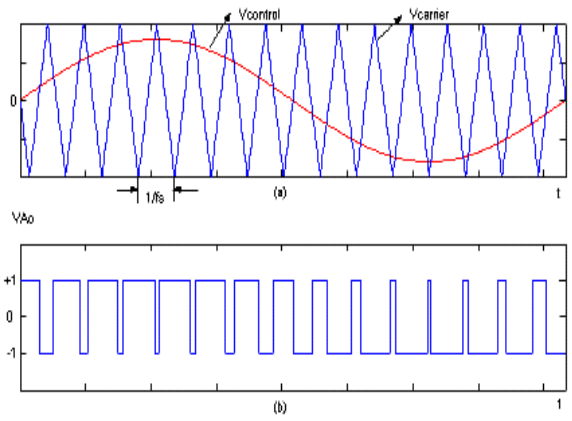

Figure 2. Description of PWM Modulation

where A_c is the amplitude of the carrier signal.

From Fourier transformation theory any time varying function $f(t)$ can be expressed as a summation of harmonic components [1]:

$$f(t) = \frac{a_o}{2} + \sum_{m=1}^{\infty}\left[a_m \cos mwt + b_m \sin mwt\right] \tag{3}$$

where

$$a_m = \frac{1}{\pi}\int_{-\pi}^{\pi} f(t)\cos mwt dwt \quad \text{m= 0, 1…,} \infty \tag{4}$$

$$b_m = \frac{1}{\pi}\int_{-\pi}^{\pi} f(t)\sin mwt dwt \quad \text{m= 1, 2…,} \infty \tag{5}$$

Based on the principle of double Fourier integral, and using equation (3) the harmonic component form can be developed for a double variable controlled waveform $f(x,y)$ as:

$$f(x,y) = \begin{cases} \frac{A_{00}}{2} + \sum_{n=1}^{\infty}\left[A_{n0}\cos nx + B_{n0}\sin nx\right] + \\ \sum_{m=1}^{\infty}\left[A_{m0}\cos mx + B_{mo}\sin mx\right] + \\ \sum_{m=1}^{\infty}\sum_{\substack{n=-\infty \\ (n\neq 0)}}^{\infty}\left[A_{mn}\cos(mx+ny) + B_{mn}\sin(mx+ny)\right] \end{cases} \tag{6}$$

where:

$$A_{mn} = \frac{1}{2\pi^2}\int_{-\pi}^{\pi}\int_{-\pi}^{\pi} f(x,y)\cos(mx+ny)dxdy \tag{7}$$

$$B_{mn} = \frac{1}{2\pi^2}\int_{-\pi}^{\pi}\int_{-\pi}^{\pi} f(x,y)\sin(mx+ny)dxdy \tag{8}$$

Or in complex form:

$$\bar{C}_{mn} = A_{mn} + jB_{mn} = \frac{1}{2\pi^2}\int_{-\pi}^{\pi}\int_{-\pi}^{\pi} f(x,y)e^{j(mx+ny)}dxdy \tag{10}$$

Replacing x by $\omega_c t+\theta_c$ and y by $\omega_o t+\theta_o$, equation (5) can be expressed in time varying form as:

$$f(t) = \begin{cases} \frac{A_{00}}{2} + \sum_{n=1}^{\infty}\left[A_{on}\cos(n[\omega_0 t+\theta_0]) + B_{on}\sin(n[\omega_0 t+\theta_0\right] + \\ \sum_{m=1}^{\infty}\left[A_{mo}\cos(m[\omega_c t+\theta_c] + b_{mo}\sin(m[\omega_c t+\theta_c])\right] + \\ \sum_{m=1}^{\infty}\sum_{\substack{n=-\infty \\ (n\neq 0)}}^{\infty}\left\{\begin{matrix} A_{mn}\cos(m[\omega_c t+\theta_c] + n(\omega_o t+\theta_o]) + \\ B_{mn}\sin(m[\omega_c t+\theta_c] + n[\omega_o t+\theta_o])] \end{matrix}\right\} \end{cases} \tag{11}$$

where the first two factors represent fundamental component and base-band harmonics, the third – carrier harmonics and the last one – the side-band harmonics.

Equation (11) gives the full guidelines on harmonic component of any given PWM scheme.

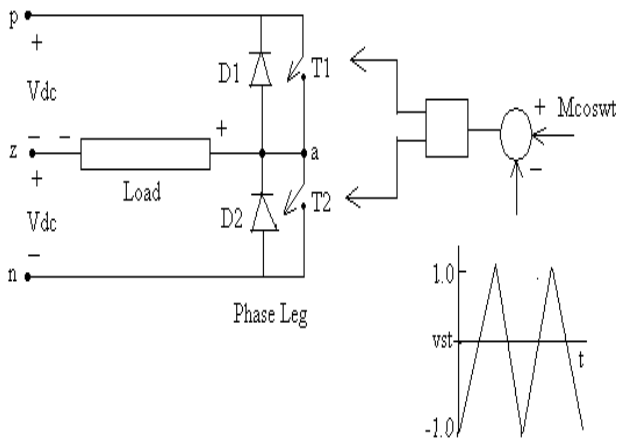

Figure 3. Naturally sampled double edge PWM one phase leg voltage source Inverter

Fig. 3 shows one phase leg of an inverter driven by a triangular wave carrier (as in Fig.2). The phase leg is switched to the upper DC rail when the reference waveform is greater than the triangular wave carrier and to the lower DC rail when the carrier waveform is greater than the reference waveform. To obtain a sinusoidal output using this modulation strategy, the reference waveform has the form:

$$v_{az} = M\cos(\omega_o t + \theta_0) = M\cos y \tag{12}$$

where: M = modulation index, 0<M<1
ω_o = target output frequency
θ_o = arbitrary output phase

Using the unit cell principal [5], the inner integral limit for naturally sampled sine triangular modulation can be derived as shown in equation (20) in which both edges are being modulated. This can be easily identified as instantaneous values of modulating reference waveform during each carrier period.

$$x_p = -\frac{\pi}{2}(1 + M\cos y) \tag{13}$$

For $f(x,y)$ changing from $+V_{dc}$ to $-V_{dc}$ (and

$$x_n = +\frac{\pi}{2}(1 + M\cos y) \tag{14}$$

For $f(x,y)$ changing from $+V_{dc}$ to $-V_{dc}$ and under the integration defined by (13) and (14) equation (15) becomes:

$$\bar{C}_{mn} = \int_{-\pi}^{\pi}\int_{-\frac{\pi}{2}(1+M\cos y)}^{\frac{\pi}{2}(1+M\cos y)} 2V_{dc}e^{j(mx+ny)}dxdy \tag{15}$$

Using equation (14) above particular harmonics for various index variables m and n can be evaluated for m=n =0 (DC offset), m=0, n.>0 (base band harmonics), m>0, n=0 (carrier harmonics), m>0, $n \neq 0$ (side band harmonics). Equation (15) is obtained by substituting the four components in equation (11) above. This equation explicitly gives the harmonic content of the phase voltage:

$$f(t) = \begin{cases} MV_{dc}\cos(\omega_0 t) + \frac{V_{dc}}{\pi}\sum_{m=1}^{\infty} J_0(mM\frac{\pi}{2})\sin(m\frac{\pi}{2})\cos(m\omega_c t) + \\ \frac{V_{dc}}{\pi}\sum_{m=1}^{\infty}\sum_{n=\pm1}^{\pm\infty}\frac{J_n(mM\frac{\pi}{2})}{m}\sin[(m+n)\frac{\pi}{2}]\cos(m\omega_c t + n\omega_0 t) \end{cases} \tag{16}$$

where: J_o, J_n = Bessel function of the first kind

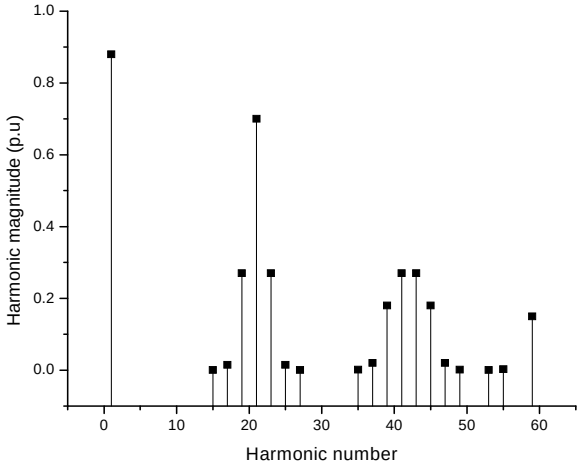

Figure 4. Theoretical results: Harmonic spectrum of SPWM with triangular carrier and modulation index = 0.9 and $f_c/f_0 = 21$

Equation (16) has the following important information:

- The first term gives the amplitude of the fundamental and shows that this is directly proportional to modulation index
- The second term shows the amplitude of the harmonic at the carrier frequency multiples of the carrier frequency and it shows that due to the presence of sin(mπ/2), no harmonics occur at even multiples of the carrier frequency.

For double edged naturally sampled PWM odd harmonic side band components around the odd multiples of carrier fundamental and even harmonic side band components around the even multiples of the carrier fundamental, are completely eliminated by the

$\sin[(m+n)\pi/2]$. This can be illustrated by theoretical SPWM model in fig. 4

3. Third Harmonic Injection PWM

A major limitation with the SPWM modulation is the reduced maximum peak fundamental output line voltage of $\sqrt{3}V_{dc}$ that can be obtained compared to the available DC link voltage. This limitation has important implication of high power high voltage UPS application since it will require the installation of a very large PV arrays, thus increase in weight of the UPS.

It is readily shown that for peak input line to line voltage of V_p, the average DC link voltage will be $3V_p/\pi$ assuming a perfect zero impedance source [6]. The maximum peak inverter output voltage will therefore be $(\sqrt{3}/2)\times(3V_p/\pi)$ or 82.7% of V_p.

From a universal representation of modulation signal $v_i(t)(i=a,b,c)$ for a three phase, the PWM modulation is as [7]:

$$v_i(t) = v_i^*(t) + e(t) \tag{17}$$

where $e(t) = \sin 3\omega t$ taking the signal amplitude to be 1

$$v_i^*(t) = \begin{cases} v_a^*(t) = M\sin(\omega_o t) \\ v_b^*(t) = M\sin(\omega_o t + 2\pi/3) \\ v_c^*(t) = M\sin(\omega_o t - 2\pi/3) \end{cases} \tag{18}$$

where M = modulation index.

For balanced three phase system:

$$v_a^*(t) + v_b^*(t) + v_c^*(t) = 0 \text{ for } e_i(t) = 0 \tag{19}$$

Hence, from above the output line to neutral voltage $v_{iN}(i=a,b,c)$ are

$$v_{aN}(t) = V_{dc}\left[M\sin\omega t + e(t)\right] \tag{20}$$

$$v_{bN}(t) = V_{dc}\left[M\sin(\omega t + 2\pi/3) + e(t)\right] \tag{21}$$

$$v_{cN}(t) = V_{dc}\left[M\sin(\omega t - 2\pi/3) + e(t)\right] \tag{22}$$

The output line-to-line voltage v_{ab}, v_{bc} and v_{ca} are:

$$v_{ab}(t) = \sqrt{3}V_{dc}\left[M\sin(\omega t + \pi/6)\right] \tag{23}$$

$$v_{bc}(t) = \sqrt{3}V_{dc}\left[M\sin(\omega t + 5\pi/6)\right] \tag{24}$$

$$v_{ca}(t) = \sqrt{3}V_{dc}\left[M\sin(\omega t + 3\pi/2)\right] \tag{25}$$

The above eq. system show that, using the third harmonic injection, the amplitude of the line-to-line voltage is √3 higher than the conventional SPWM technique.

From (23), (23) and (25) above it is clear that injected harmonic $e(t)$ do not appear in the line-to-line output voltage of the inverter. Thus $e(t)$ is called zero sequence signal and can be obtained by:

$$e(t) = (1/3)[v_a(t)+v_b(t)+v_c(t)]$$

From above analysis, the inner integral limits for PWM using simple sinusoidal reference is known and thus strategies which use third harmonic injection to improve the harmonic performance and increase the modulation depth of the modulation process. This can be readily accommodated by changing such limits to:

$$x_p = -\frac{\pi}{2}(1 + M\cos y' + A\cos 3y) \tag{26}$$

$$x_n = +\frac{\pi}{2}(1 + M\cos y' + A\cos 3y) \tag{27}$$

This gives the third harmonic injection PWM equation as;

$$f(t) = \frac{4V_{dc}q}{\pi}\left\{\begin{array}{l} J_0(\frac{q\pi A}{2})J_n(\frac{q\pi M}{2})\sin([m+n]\frac{\pi}{2}) \\ +J_0(\frac{q\pi M}{2})J_h(\frac{q\pi A}{2})\sin([m+h]\frac{\pi}{2})\Big|_{3h=|n|} \\ +J_k(\frac{q\pi M}{2})J_h(\frac{q\pi A}{2})\sin([m+h+k]\frac{\pi}{2})\Big|_{k+3h=|n|} \\ +J_k(\frac{q\pi M}{2})J_h(\frac{q\pi A}{2})\sin([m+h+k]\frac{\pi}{2})\Big|_{k-3h=|n|} \\ J_k(\frac{q\pi M}{2})J_h(\frac{q\pi A}{2})\sin([m+h+k]\frac{\pi}{2})\Big|_{3k-h=|n|} \end{array}\right\} \tag{28}$$

where $q = m+n\omega_o/\omega_c$

A = Third harmonic magnitude

J_k, Jh = Bessel functions $(1\le k\le\infty)$, $(1\le h\le\infty)$

From equation (28) it is seen that due to the presence of $\sin[m+n]\pi/2$ odd harmonic side band components around the odd multiples of carrier fundamental and even harmonic side band components around the even multiples of the carrier fundamental, are completely eliminated just as SPWM but due to absence of $\sin(m\pi/2)$, there are harmonics at even multiples of the carrier frequency and thus the THD of THIPWM is higher than SPWM, this shows analytically that SPWM is a preferred control technique for UPS powering sensitive loads. This is illustrated in figure 5.

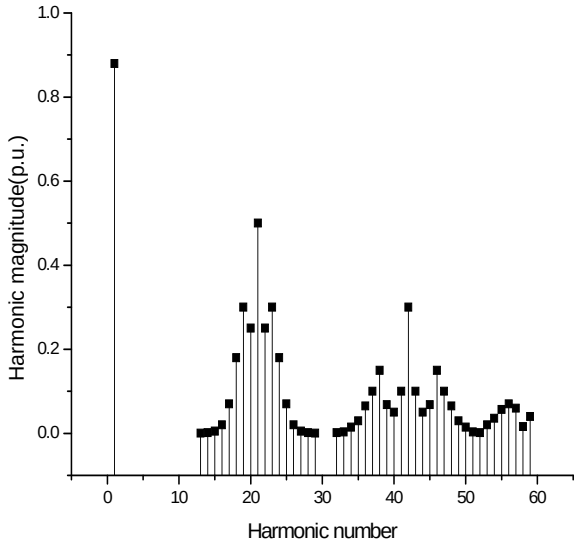

Figure 5. Theoretical results: Harmonic spectrum of THIPWM with triangular carrier and modulation index = 0.9 and $f_c/f_0 = 21$

4. Simulation Results

To verify the performance of the proposed UPS inverter, the complete system was simulated using MATLAB SIMULINK on 200 KVA UPS inverter [8]. The SPWM model of the UPS for simulation is as shown in figure 5. The inverter model is a three phase three wire topology employing three level inverter. The model uses voltage source inverter (VSI).The system parameters for simulation are shown in table 1.

The block diagram of instantaneous feedback control is shown is fig 7 Ud_ref is the reference signal for SPWM for THIWPM it consist of pure sine wave and injected third harmonic to ensure the best effect of HIPWM the injected third harmonic should be phase locked with modulating waveform. In order to improve the dynamic performance of the UPS inverter under varying load conditions, the PWM control model is combined with feedback loops having both current and voltage controllers. PI controllers compensators are included in each of the voltage and current controllers to guarantee robustness of the system. The voltage major loop controller assures sinusoidal output voltage and stabilizes the system. In this model the capacitor voltage, inductor current and load current are used as feedback control signals. The addition of load current instead of the usual inductor current is based on the fact that performance of UPS can be considerably improved if the load current is effectively controlled. The load current loop is also important in attenuating the effect disturbances in the load. For PWM generator shown in fig. 8, Phase disposition PWM which offers improved harmonic performance is applied [9]. For a three level inverter where N=3 (number is levels), two carriers that are in phase across all bands are used.

Table 1
System hardware parameter

Symbol	Parameter	Value
V_g	AC source voltage (grid voltage)	400V, 50 HZ
L_c	Input filter inductance	0.27 mH
C_s	Input filter capacitance	300μF
C_{dc}	DC link capacitance	$C_{dc}1=C_{dc}2=0.042F$
V_{dc}	DC bus voltage from PV array	810V
L_O	Output filter inductance	0.27mH
C_O	Output filter capacitance	40 KVAR
	Rated load	200KVA

4.1 SPWM Simulation Results

The results for an inverter controlled by SPWM are shown in figures 9 and 10.

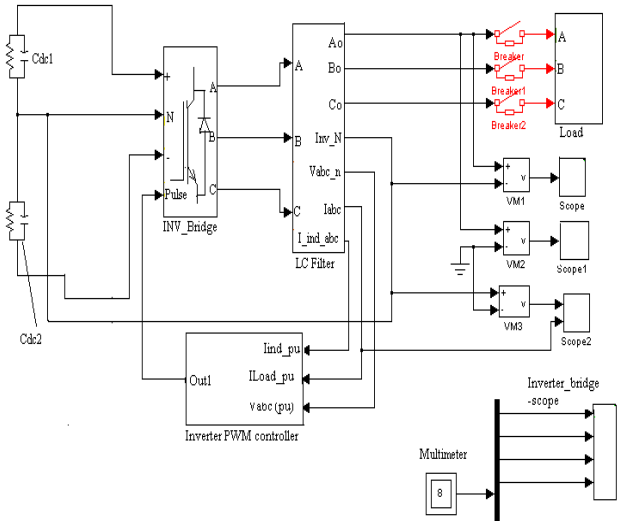

Figure 6. Simulation model

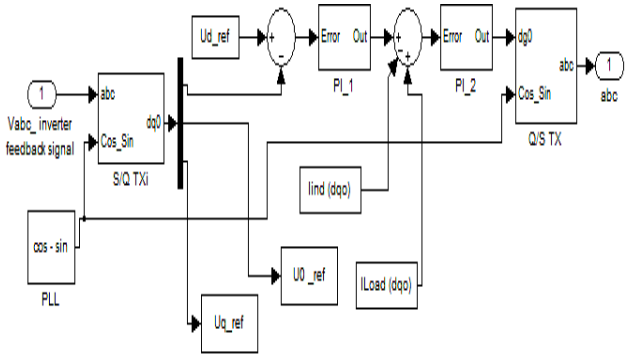

Figure 7. Instantaneous feedback control of the inverter

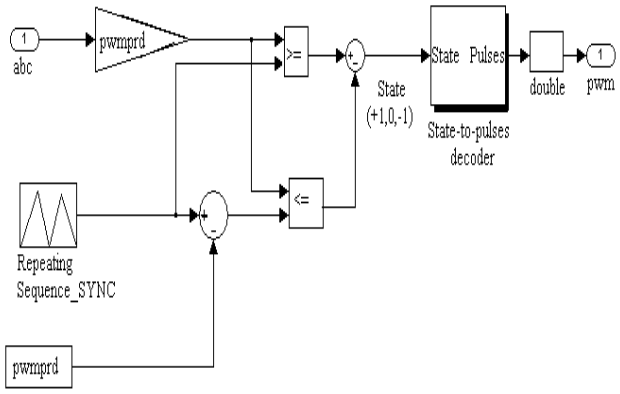

Figure 8. Three level PWM generator

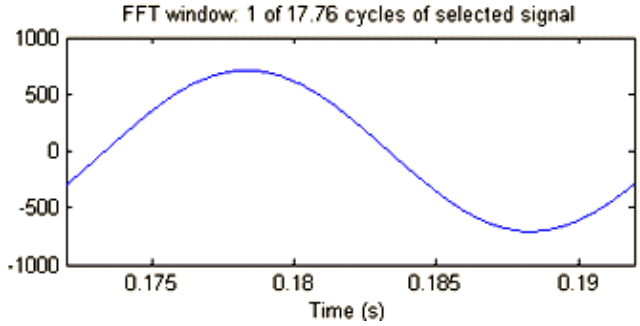

(a)

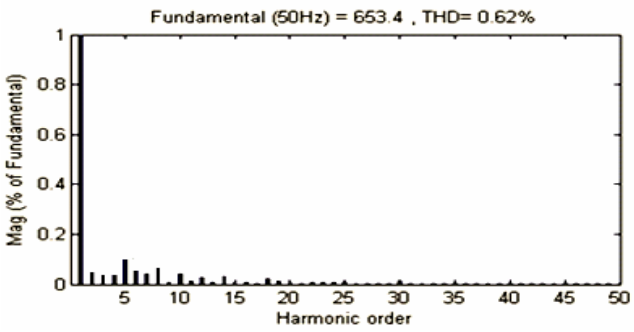

(b)

Figure 9. (a) Line voltage waveform for SPWM UPS inverter (b) its respective harmonic spectrum

As can be seen from harmonic spectrum of figures 9(b) and 10(b) the THDs of the two modulation methods meet the required UPS specification which is supposed to be less than 3% for linear loads. And less than 5% for non linear loads as can seen from figure 6 (c)

The THD of output voltage for SPWM simulated waveforms are lower than that of THIPWM; this makes the proposed SPWM model better choice for UPS powering highly sensitive loads, it is also worth to note that the high frequency harmonics found which can be seen around harmonic order of 100, 200, and 300 results from the PWM switching harmonics. These harmonics occur at $n = m_f \pm 2$ for naturally sampled sinusoidal PWM. Where m_f = 100 for the proposed model.

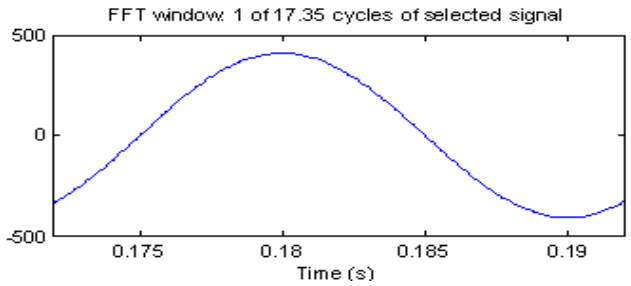

(a)

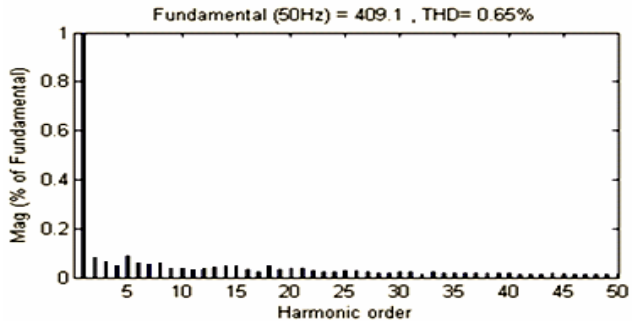

(b)

Figure 10. (a) Phase voltage waveform for SPWM UPS inverter (b) its respective harmonic spectrum

4.2 THIPWM Simulation Results

In figure 11, the linear balanced load was used for testing the effectiveness of Third Harmonic Injection PWM control technique.

.

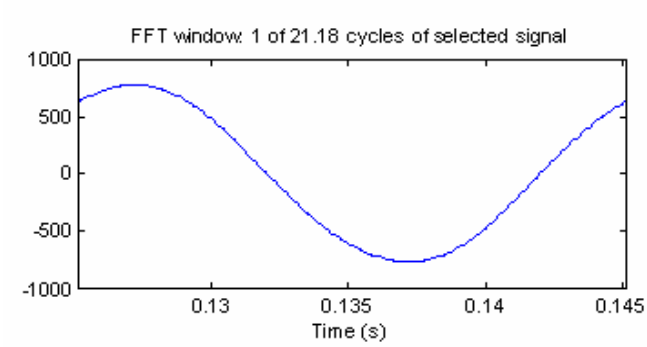

(a)

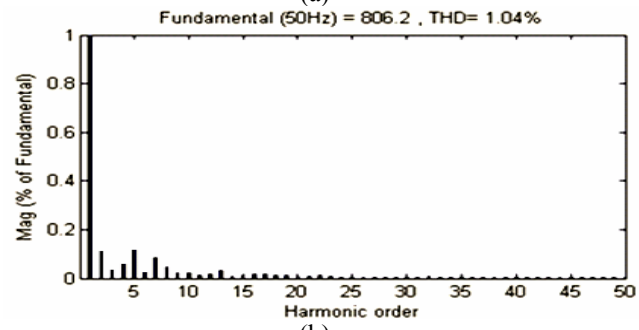

(b)

Figure 11. (a) Line voltage waveforms for THIPWM UPS inverter (b) its respective harmonic spectrum

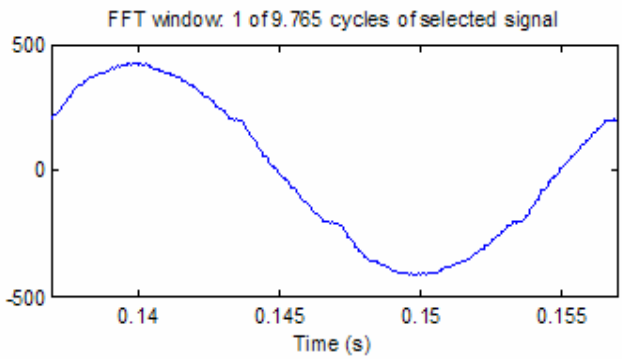

(a)

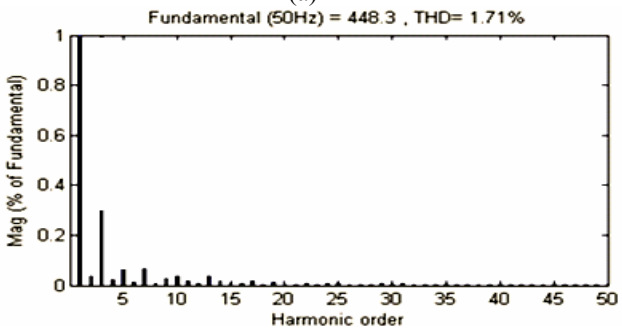

(b)

Figure 12. (a) Phase voltage waveforms for THIPWM UPS inverter (b) its respective harmonic spectrum

The conversion factor which is defined as:

$$CF = \frac{V_{LL,1p}}{V_{dc}}\bigg|_{m=1}$$

where $V_{LL,1p}$ denotes the peak value of the fundamental line to line output voltage of the inverter), of THIPWM modulation is higher, this implies that utilization of DC bus using THIPWM is better than that of SPWM. This as explained earlier is due to addition of 17% third harmonic to the reference voltage. This reduces the peak size of the envelope of each phase leg voltage and hence the modulation index m_i can be increased beyond m_i=1.0 without moving into over modulation. This makes THIPWM a preferred choice in high voltage high power UPS. Under balanced operating condition, third order current harmonics cannot flow and thus third – order voltage harmonics are neutralized in line to line voltage (figure 8(b)) , Third harmonic is present in phase voltage which results in higher THD in figure 12(b).

5. Conclusion

SPWM control technique with triangular wave carrier has been extensively analyzed and compared to other THIPWM control technique, based on the simulated results SPWM modulation is suitable for most applications in UPS inverter which in most cases is used for supplying power to highly sensitive loads.

It has also been demonstrated by simulation that for maximum power utilization of DC bus voltage, the proposed third harmonic injection PWM results in maximum fundamental output voltage, this is a desirable feature for high power high voltage UPS.

References

[1] M. Carpito, M. Mazzucchelli, S.Savio and G. Sciutto, A new PWM control system for UPS using hysteresis comparator, *IEEE, IAS annual meet. Conf., Rec.* 1987, pp. 749 – 754

[2] Hongying Wu, Dong Ling, Dehua Zhang, Kaiwei Yao and Jinfa Zhang, A current – mode control technique with instantaneous inductor current feedback for UPS inverter, *IEEE Trans. On PESC,* 1999, PP. 951- 957

[3] J.F. Chen and C.L.Chu, A combination of voltage – controlled and current – controlled PWM inverter for UPS parallel operation, *IEEE Transaction Power Elect., vol. 10,* no. 5, Sept. 1995, pp. 547- 558

[4] Mohan, Underland and Robbins, *Power Electronics: converters, applications, and design* (3rd edition. A John Wiley & Sons publication, 200).

[5] D.G.Holmes and Thomas A.Lipo, *Pulse Width Modulation for Power Converters –principles and practices* (IEEE press series, A John Wiley & Sons inc. publication, 2003)

[6] A. M. Hava, R. J. Kerkman, and T. A. Lipo, Simple analytical and graphical methods for carrier based PMW VSI Drives, *IEEE Trans. on Power Electronics***,** *Vol. 14,* No. 1, Jan., 19998.

[7] T.A. Lipo and A.M. Hava, A high- performance generalized discontinuous PWM algorithm*,IEEE Transactions on Ind. Appl., Vol. 33*, No.5, Sep./Oct. 1997 pp. 1059-1071

[8] Jack Little and Cleve Moler, *MATLAB 6.5-Numerical Computation Software* (Mathworks, Inc., 2002)

[9] G. Carrara, S. Gardella, M. Marchesoni, R. Salutari and G. Sciutto, A new multilevel PWM method: a theoretical analysis, *IEEE Trans. on power electronics, vol. 7*, July, 1992 pp. 497 -505.